JOURNAL OF MATERIALS SCIENCE 14 (1979) 831–840

# Tensile strength of composites with brittle reaction zones at interfaces

SHOJIRO OCHIAI, YOTARO MURAKAMI
*Department of Metallurgy, Faculty of Engineering, Kyoto University, Kyoto 606, Japan*

A theoretical model of the longitudinal strength of brittle fibre-reinforced composites with brittle reaction zones was presented for both cases of strongly and weakly bonded fibre/brittle zone interfaces. First, on the basis of the fracture mechanics, a model of the strength of the fibres coated with strongly adhering brittle zones was proposed as a function of the thickness of the brittle zones. Next, the conditions under which debonding occurs at the interfaces were investigated with the aid of the shear lag analysis proposed by Cox. The theoretical model was then examined using composites with strongly and weakly bonded interfaces. The proposed model agreed fairly well with the experimental results. Finally, the permissible thickness of the brittle zone below which no reduction in fibre strength appears was calculated, using the proposed theory, under the condition of strong interfacial bonding, for carbon, boron and silicon carbide fibres which are of practical use. The calculated values of the thickness were smaller than 1 $\mu$m.

## Nomenclature

$z$ = distance from broken end of brittle zone
$a$ = radius of fibre
$b$ = radius of composite employed in theory consisting of two components (fibre and brittle zone)
$c$ = thickness of brittle zone
$V$ = volume fraction in two-component composite
$V'$ = volume fraction in three-component composite employed in application
$K_c$ = fracture toughness of fibre
$G_c^*$ = critical strain energy release rate of fibre
$E$ = Young's modulus
$G$ = shear modulus
$\sigma$ = tensile stress
$\tau_i$ = interfacial shear stress
$\tau_{i,max}$ = maximum interfacial shear stress
$\tau^\Delta$ = interfacial shear strength
$\sigma_c$ = tensile strength of two-component composite
$\sigma_c'$ = tensile strength of three-component composite
$\sigma_{co}'$ = tensile strength before annealing of three-component composite
$\sigma_m^*$ = yield stress of matrix
$\sigma_b$ = tensile stress in brittle zone
$\sigma_{bu}$ = tensile strength of brittle zone
$\epsilon_f$ = fibre strain at $z = 0$
$\epsilon_f^*$ = fibre strain at $z = 0$, at which notch effect arises
$\epsilon_f^\Delta$ = fibre strain at $z = 0$, at which debonding occurs
$\epsilon_f'$ = fibre strain at $z = 0$ at fracture of brittle zone
$\epsilon_{fu}$ = fracture strain of bare fibre
$\epsilon_{bu}$ = fracture strain of brittle zone
$\bar{\epsilon}_f$ = fracture strain of fibre at $z = 0$
$c_I$ = thickness of brittle zone below which fibre is not degraded = maximum permissible thickness of brittle zone in the case of strong fibre/brittle zone interface
$c_{II}$ = thickness of brittle zone beyond which fibre fractures as soon as brittle zone fractures
$u$ = displacement
$H$ = $2G_b/a^2 \ln(b/a)$
$\beta$ = $HE_c/E_fE_bV_b$
$\rho$ = root radius of notch
$l'$ = average length of segmented brittle zone
$\gamma_s$ = fracture surface energy
$a_o$ = lattice spacing

Subscripts

c = composite
f = fibre
b = brittle zone
m = matrix

## 1. Introduction

In artificial composites, interfacial chemical reaction between fibre and matrix often takes place during preparation and/or service. The reaction has been known as one of the causes of reducing the strength of composites. In most reported cases of the reaction, the formed reaction zones are brittle and fracture at small strains, thus forming circumferential notches. The formed notches hasten fracture of the fibres, resulting in loss of composite strengths [1–4]. However, if the interfacial bonding between the fibres and the brittle zones is weak and, therefore, debonding occurs during deformation, the strength of the fibres will not be reduced because debonding will cause blunting of the notch-tip. This behaviour is inferred by the fact that transverse cracks in weakly bonded composites are able to be arrested by splitting [5–9] and the strength of such composites obeys the rule of mixtures [6, 8].

For the case of strong interfacial bonding between the fibres and the brittle zones, Heitman *et al.* [2] and Metcalfe and Klein [4] have attempted to explain the effect of brittle zones on the strength of composites, using Griffith's theory and the idea of stress concentration factor, respectively. Their theories explained well their experimental results. However, their theories failed to describe the case of weak interfacial bonding. In general, the strength of composites is strongly affected by the interfacial bonding strength, so that a further study including both the cases of weak and strong interfacial bondings is needed.

In this paper, a theoretical model of the strength of the fibres is first proposed as a function of thickness of the brittle zones for the case of strongly bonded fibre/brittle zone interface. Next, the conditions under which debonding occurs for a weakly bonded interface are theoretically made clear. The proposed model is then examined using Metcalfe's result [4] on boron fibre/brittle zone/titanium alloy matrix composites with strong interfacial bonding and our results on tungsten fibre/brittle zone/aluminium matrix composites with weak interfacial bonding. Finally, for the case of strong interfacial bonding, the permissible thickness of the brittle zone, below which no degradation effect of the brittle zone on the fibre strength exists, is calculated for carbon, boron and silicon carbide fibres which are of practical use.

## 2. Theory

To analyse the effect of a formation of a notch, a two-component composite cylinder of an inner core of fibre and an outer case of brittle reaction zone, shown in Fig. 1, is employed. The radii of the fibre and composite are shown by $a$ and $b$, respectively, the thickness of the brittle zone by $c(= b - a)$, and the distance from the broken end of the zone by $z$. When the brittle zone fractures and a notch is formed in an early stage of deformation, the composite is able to be regarded as a rod with a circumferential notch. If the interface is strong enough to permit the formed notch to extend into the fibre, a notch effect arises, resulting in a reduction in fibre strength. On the other hand, if the exerted shear stress on the interface exceeds the interfacial shear strength, debonding occurs and leads to no loss in fibre strength. To determine whether the notch effect or debonding occurs, we calculate the fibre strains at the notched section ($z = 0$ in Fig. 1) for the notch effect and debonding, and then compare them. Denoting the strain of the fibre at $z = 0$, at which notch effect arises, by $\epsilon_f^*$, and that at which debonding arises

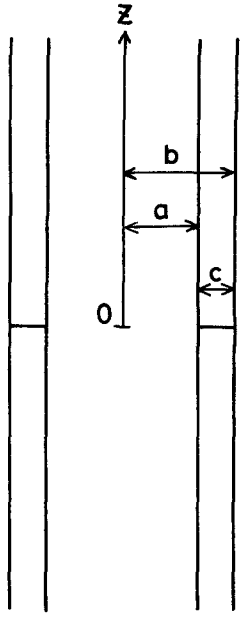


*Figure 1* Model for the analysis of the effects of formation of a notch on the tensile behaviour of composites.

by $\epsilon_f^{\Delta}$, we can expect that the notch effect will occur prior to debonding if $\epsilon_f^* < \epsilon_f^{\Delta}$, and debonding prior to the notch effect if $\epsilon_f^{\Delta} < \epsilon_f^*$. In Section 2.1 we deal with the case of a strong interface which allows the formed notch to extend into the fibre. In Section 2.2, we deal with the case of a weak interface which in some cases prevents the notch from extending into the fibre. In the following model we assume, for simplicity, that the fracture strain of the brittle zone is constant for the whole range of $c$.

## 2.1. Notch effect

The fracture toughness $K_c$ for a rod with a circumferential notch is given by [10]

$$K_c = \sigma_{net}\sqrt{(\pi c)}F(a/b), \tag{1}$$

where $\sigma_{net}$ is the stress in the fibre at $z = 0$ and $F(a/b)$ is a function of $a/b$, given by [10]

$$F(a/b) = \tfrac{1}{2}\sqrt{(a/b)}[1 + \tfrac{1}{2}(a/b) + \tfrac{3}{8}(a/b)^2 - 0.363(a/b)^3 + 0.731(a/b)^4]. \tag{2}$$

The critical strain energy release rate of the fibre, $G_c^*$, for plane stress is given by [11]

$$G_c^* = K_c^2/E_f, \tag{3}$$

where $E_f$ is the Young's modulus of the fibre. As $\sigma_{net}$ is equal to $\epsilon_f E_f$, where $\epsilon_f$ is the fibre strain at $z = 0$, the fracture strain of the fibre at $z = 0$, $\epsilon_f^*$, is represented from Equations 1 and 3 by

$$\epsilon_f^* = \frac{K_c}{E_f F(a/b)\sqrt{(\pi c)}} \tag{4}$$

$$= \frac{1}{F(a/b)}\sqrt{\left(\frac{G_c^*}{E_f \pi c}\right)}. \tag{5}$$

As the fibre strain at fracture of the brittle zone is $\epsilon_{bu}E_c/E_f V_f$ at $z = 0$, where $E_c$ is the Young's modulus of the composite and $\epsilon_{bu}$ is the fracture strain of the brittle zone, we define

$$\epsilon_f' = \epsilon_{bu}E_c/E_f V_f. \tag{6}$$

Comparing the calculated values of $\epsilon_f^*$ with $\epsilon_f'$ and the fracture strain of the bare fibre $\epsilon_{fu}$, we can describe the variation of the fracture behaviour as a function of $c$. For a better description, we divide the variation into three regions, as shown in Fig. 2.

Region I: when the brittle zone is thin and the effect of the intrinsic defects in the fibre is stronger than that of the newly formed notch, the fibre is able to maintain its own full strength. This region corresponds to the calculated region of $\epsilon_f^* > \epsilon_{fu}$. In this region, the fibre is not degraded by the formed notch, and the composite strength, $\sigma_c$, is given by

$$\sigma_c = \epsilon_{fu}E_f V_f. \tag{7}$$

With further increase in $c$, the effect of the formed notch becomes more predominant than that of the intrinsic defects in the fibre, and the fibre strength begins to decrease at $c = c_I$. The value of $c_I$ is calculated by substituting $\epsilon_f^* = \epsilon_{fu}$ into Equation 5,

$$c_I\, F(a/b)^2 = G_c^*/\pi\epsilon_{fu}^2 E_f. \tag{8}$$

The value of $c_I$ is regarded as the maximum permissible thickness below which the fibre is not degraded.

Region II: the strength of the fibre decreases with increasing $c$ and the fracture strain of the fibre is given by Equation 5. This region corresponds to the range of $\epsilon_f' < \epsilon_f^* < \epsilon_{fu}$. In this region the fibre is able to deform after the formation of the notch until the stress level is favourable for the notch to extend. In this region, $\sigma_c$ is given by

$$\sigma_c = \epsilon_f^* E_f V_f = \frac{V_f}{F(a/b)}\sqrt{\left(\frac{E_f G_c^*}{\pi c}\right)}. \tag{9}$$

Region III: when the formed notch is large enough to break the fibre immediately, the fibre fractures as soon as the brittle zone fractures. This region corresponds to the range of $\epsilon_f^* < \epsilon_f'$. In the ordinary composite, the fracture strain of the composite never falls below $\epsilon_{bu}$, since the notch is formed at first at $\epsilon_{bu}$. In this region $\sigma_c$ is given by

$$\sigma_c = \epsilon_{bu}E_c. \tag{10}$$

The strength $\sigma_c$ remains nearly constant with further increase in $c$ since, in general, $c$ is so small that $V_f$ decreases very little. The thickness at which region III initiates, $c_{II}$, is given by

$$\epsilon_f^* = \epsilon_f', \tag{11}$$

namely, $c_{II}$ satisfies Equation 12.

$$c_{II}\, F(a/b)^2 = V_f^2 G_c^* E_f/\pi(\epsilon_{bu}E_c)^2. \tag{12}$$

In Fig. 2, the regions stated above are described schematically. Thus $\sigma_c$ and fracture strain of the fibre at $z = 0$, $\bar{\epsilon}_f$, are described as a function of $c$.

Metcalfe and Klein [4] have already investigated the strength of composites (B/Ti40A and B/Ti75A) with a reaction zone of various thicknesses using stress concentration factors at the tip

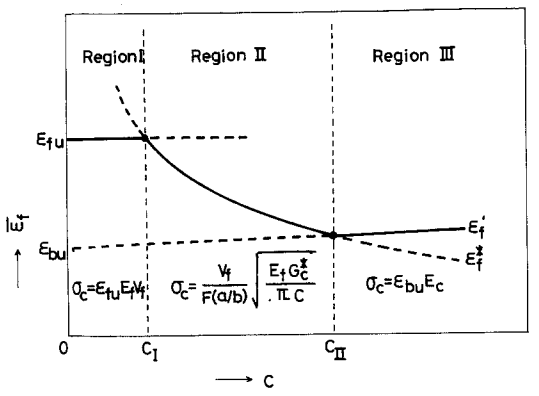


*Figure 2* Variations of $\bar{\varepsilon}_f$ and $\sigma_c$ with $c$ under the condition of strong interfacial bonding between the fibre and the brittle zone.

of the formed notch. Our theory yields similar results to theirs but differs by the following two points.

(i) We have applied fracture mechanics to the composite with a circumferential notch, while Metcalfe and Klein applied the idea of stress concentration at the notch tip.

(ii) In their theory, Metcalfe and Klein used the stress concentration factor $K = B(c/\rho)^{1/2}$, where $\rho$ is the root radius of the notch, and assumed that $B = 1$ and $\rho = 0.3$ nm (minimum cell size of the reaction zone in B/Ti40A and B/Ti75A composites). However, these assumptions are arbitrary. In our theory, these assumptions are not used. Our theory allows us to predict the variation of $\sigma_c$ as a function of $c$ without such assumptions.

In this section, interfacial shear strength was assumed to be strong enough for the interface not to fail. In ordinary composites, the interface often fails during deformation. The next section deals with such a case.

## 2.2. Interfacial debonding

To determine the exerted shear stress at the interface, we first calculate the stress distributions in the fibre and the brittle zone along the $z$-axis under the conditions where a notch is already formed. Following the shear lag analysis of Cox [12], the variation of the fibre stress $\sigma_f(z)$ along the $z$-axis due to the transfer of load from the fibre to the brittle zone is written by

$$\frac{d\sigma_f(z)}{dz} = H(u_f - u_b), \tag{13}$$

where $H$ is a constant (defined later) and $u_f$ and $u_b$ are displacements of the fibre and the brittle zone, respectively. Differentiating Equation 13, we have

$$\frac{d^2\sigma_f(z)}{dz^2} = H\left(\frac{du_f}{dz} - \frac{du_b}{dz}\right) = H\left[\frac{\sigma_f(z)}{E_f} - \frac{\sigma_b(z)}{E_b}\right], \tag{14}$$

where $\sigma_f(z)$, $\sigma_b(z)$ are stresses of the fibre and the brittle zone at $z = z$, and $E_f$, $E_b$ are the Young's moduli of the fibre and the brittle zone, respectively. If the strain of the fibre is $\epsilon_f$ at $z = 0$, the load borne by the cross-section at $z = 0$ is

$$\sigma_c(z = 0) = \epsilon_f E_f V_f. \tag{15}$$

At $z = z$, the load borne by the composite is

$$\sigma_c(z = z) = \sigma_f(z)V_f + \sigma_b(z)V_b \tag{16}$$

As the load borne by the composite must be constant at any cross-section, $\sigma_b(z)$ is obtained from Equations 15 and 16.

$$\sigma_b(z) = [\epsilon_f E_f V_f - \sigma_f(z)V_f]/V_b \tag{17}$$

Substituting Equation 17 into Equation 14, we have

$$\frac{d^2\sigma_f(z)}{dz^2} = H\left[\frac{E_c}{E_f E_b V_b} \cdot \sigma_f(z) - \frac{\epsilon_f E_f V_f}{E_b V_b}\right], \tag{18}$$

where $E_c = E_f V_f + E_b V_b$. The solution of Equation 18 subject to the boundary condition $\sigma_f(z = 0) = \epsilon_f E_f$ is

$$\sigma_f(z) = \frac{\epsilon_f E_f E_b V_b}{E_c} \cdot \exp(-\sqrt{\beta}z) + \frac{\epsilon_f E_f^2 V_f}{E_c}, \tag{19}$$

where $\beta = HE_c/E_f E_b V_b$. Substituting Equation 19 into Equation 17, we have

$$\sigma_b(z) = \frac{\epsilon_f E_f E_b V_f}{E_c}[1 - \exp(-\sqrt{\beta}z)]. \tag{20}$$

The constant $H$ is estimated by treatment similar to that of Aveston and Kelly [13], and is given by

$$H = 2G_b/a^2 \ln(b/a) \tag{21}$$

where $G_b$ is the shear modulus of the brittle zone.

The interfacial shear stress, $\tau_i$, is calculated from Equation 22:

$$\tau_i = \frac{\pi(b^2 - a^2)}{2\pi a} \cdot \frac{d\sigma_b(z)}{dz} = \frac{a\epsilon_f E_f E_b V_b \sqrt{\beta}}{2E_c} \exp(-\sqrt{\beta}z). \tag{22}$$

The maximum value, $\tau_{i,max}$, arises at $z = 0$ and is given by

$$\tau_{i,max} = \frac{a\epsilon_f E_f E_b V_b \sqrt{\beta}}{2E_c}. \quad (23)$$

When $\tau_{i,max}$ exceeds the interfacial shear strength, $\tau^{\Delta}$, debonding occurs. The conditions under which debonding occurs are obtained for the following three cases.

Case (a): debonding occurs as soon as the brittle zone fractures, if the interfacial bonding is extremely weak. In this case, as the fibre strain in the notched section ($z = 0$) is given by Equation 6, we have $\tau_{i,max}$ at the fracture of the brittle zone

$$\tau_{i,max} = a\epsilon_{bu}E_b V_b \sqrt{\beta}/2V_f \quad (24)$$

by substituting Equation 6 into Equation 23. If the value of $\tau_{i,max}$ given by Equation 24 is higher than $\tau^{\Delta}$, debonding occurs as soon as the brittle zone fractures. This condition is written as

$$\tau_{i,max} = a\epsilon_{bu}E_b V_b \sqrt{\beta}/2V_f > \tau^{\Delta}. \quad (25)$$

After debonding, the fibre deforms similar to the bare fibre, and thus the fracture strain of the fibre is always $\epsilon_{fu}$. Reduction in fibre strength due to the notch effect never occurs.

Case (b): the composite is able to be stretched without debonding until $\tau_{i,max}$ given by Equation 23 exceeds $\tau^{\Delta}$, if

$$\tau^{\Delta} > a\epsilon_{bu}E_b V_b \sqrt{\beta}/2V_f. \quad (26)$$

At debonding, the fibre strain at $z = 0$, $\epsilon_f^{\Delta}$, is given by Equation 27, by substituting $\epsilon_f = \epsilon_f^{\Delta}$ and $\tau_{i,max} = \tau^{\Delta}$ into Equation 23.

$$\epsilon_f^{\Delta} = 2E_c\tau^{\Delta}/aE_f E_b V_b \sqrt{\beta}. \quad (27)$$

In this case, if $\epsilon_f^*$ is smaller than $\epsilon_f^{\Delta}$, the notch effect predominates over debonding and the fibre strength is reduced. On the other hand, if $\epsilon_f^{\Delta}$ is smaller than $\epsilon_f^*$, debonding predominates over the notch effect and thus the fibre strength does not decrease.

Case (c): when $\tau^{\Delta}$ is large enough and the value of $\epsilon_f^{\Delta}$ given by Equation 27 is always larger than $\epsilon_{fu}$, the composite deforms to fracture without debonding. This condition is written as

$$\epsilon_{fu} < 2E_c\tau^{\Delta}/aE_f E_b V_b \sqrt{\beta}. \quad (28)$$

In this case, the strength of the composite is such as that shown already in Section 2.1.

## 3. Application

First, it should be noted that the prime ($'$) is used to distinguish the composite strength and volume fractions of the components in real composites consisting of three components (fibre, brittle zone and matrix) from those of the two-component composite employed in the former sections.

### 3.1. Application to B/Ti40A and B/Ti75A composites

We will apply our theory to B/Ti40A and B/Ti75A composites whose data have been reported in detail by Metcalfe and Klein [4]. They have presented collected data on the tensile strength of these composites with various thicknesses of the brittle zone ($TiB_2$), and also normalized the strengths, $\sigma_c'$, with respect to the strength before annealing, $\sigma_{co}'$, as shown in Fig. 3, where $\sigma_{co}'$ is 858 MPa for B/Ti40A composite and 973 MPa for B/Ti75A. It was considered that these composites had strong interfaces, because if debonding had occurred, the reductions in composite strengths shown in Fig. 3 should not have taken place.

The $\sigma_c'$ for each region mentioned in Section 2.1 is written as follows:

$$\sigma_c' = \epsilon_{fu}E_f V_f' + \sigma_m^* V_m' \quad \text{for region I} \quad (29)$$

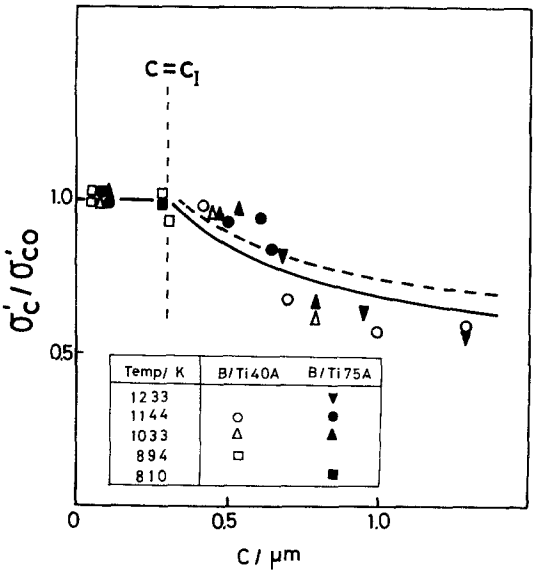


*Figure 3* Variations of $\sigma_c'/\sigma_{co}'$ of B/Ti40A and B/Ti75A composites with $c$ (after Metcalfe and Klein [4]). The temperatures refer to the annealing temperatures. The solid and dotted curves represent the theoretical values for B/Ti40A and B/Ti75A composites, respectively.

$$\sigma'_c = \frac{V'_f}{F(a/b)}\sqrt{\left(\frac{E_f G_c^*}{\pi c}\right)} + \sigma_m^* V'_m \quad \text{for region II} \tag{30}$$

$$\sigma'_c = \epsilon_{bu}(E_f V'_f + E_b V'_b) + \sigma_m^* V'_m \quad \text{for region III,} \tag{31}$$

where $V'_f$, $V'_b$ and $V'_m$ are the volume fractions of the fibre, brittle zone and matrix, respectively, in the real composites. According to Metcalfe and Klein [4], $V'_f$ and $V'_m$ before annealing are 0.25 and 0.75 respectively. $\sigma_m^*$ is the yield strength of the matrix which has been reported to be 364 MPa for Ti40A and 549 MPa for Ti75A. In the following calculations, the values of $V'_f$, $V'_b$ and $V'_m$ after annealing were taken to be $0.25(a/a+c)^2$, $0.25[1-(a/a+c)^2]$ and 0.75, respectively, and $b(=a+c)$ was taken to be 50 $\mu$m of the original fibre radius.

No value for $G_c^*$ of the boron fibre has, unfortunately, been reported to date. Therefore, we deduced the value of $G_c^*$ as follows. Fig. 3 shows that, for $c < 0.3\,\mu$m, $\sigma'_c/\sigma'_{co}$ remains constant (unity), but for $c > 0.3\,\mu$m, it decreases. Therefore, we can regard the value of 0.3 $\mu$m as $c_I$. In this case $c_I$ should satisfy

$$\frac{\sigma'_c}{\sigma'_{co}} = \left[\frac{V'_f}{F(a/a+c_I)}\sqrt{\left(\frac{E_f G_c^*}{\pi c_I}\right)} + \sigma_m^* V'_m\right] \Big/ \sigma'_{co} = 1. \tag{32}$$

Substituting the above values of $\sigma_m^*$, $\sigma'_{co}$ and $V'_m$ the equations of $V'_f$ and $V'_b$ which are functions of $c$, and the reported values of $E_f = 412$ GPa, $E_b = 530$ GPa, $\epsilon_{fu} = 0.0060$[4], for B/Ti40A composite, into Equation 32 we obtained $G_c^* = 15.8\,\mathrm{J\,m^{-2}}$.

$\sigma'_c/\sigma'_{co}$ versus $c$ curves were calculated theoretically as a function of $c$. The value of $c_{II}$ was also calculated to be 1.5 $\mu$m by substituting $\epsilon_{bu} = 0.0025$ [4], $b = 50\,\mu$m and $a = 50\,\mu\mathrm{m} - c_{II}$ into Equation 12. The calculated results were superimposed on the data in Fig. 3 where the solid and dotted curves refer to $\sigma'_c/\sigma'_{co}$ versus $c$ curves for B/Ti40A and B/Ti75A composites, respectively.

As a whole, the calculated curves agree fairly well with the measured ones. However, some discrepancy between the measured and calculated curves might arise from the following two reasons. (i) The tensile strengths and fracture strains of the fibre and the reaction zone might decrease with advancing interfacial reaction. The brittle zone is considered to become weaker with increasing thickness since the thicker the zone, the more defects it has. The fibre is also considered to be degraded since W and B react in the fibre [14]. The reductions in $\epsilon_{fu}$ and $G_c^*$ should lead to weakening of the composites, although it was assumed in the calculation that the fibre and the brittle zone maintain identical properties even after severe interfacial reaction. (ii) In our theory, static extension of notches was assumed. However, this may be an over simplification.

Although our theory is based on the simple static extension of notches, it is believed that, if the variations of $\epsilon_{fu}$ and $G_c^*$ with advancing interfacial reaction are taken into consideration, the strength of the composites is able to be described more precisely.

Our theory explains well the experimental data for region I and the initial part of region II where the changes in properties of the fibre and the brittle zone are comparatively small and the formed notch does not extend until the stress level is favourable. This fact enables us to predict the permissible thickness ($c_I$) of the reaction zone for various fibre materials. In Section 3.3, this thickness will be calculated for some promising fibres.

### 3.2. Application to W/Al composite

As the as-supplied tungsten fibres with a nominal diameter of 500 $\mu$m are ductile and fail by necking, they were made brittle by annealing in vacuum at 1573 K for 5 h. The W/Al composite with an original $V'_f = 0.20$ was fabricated by a vacuum hot-pressing technique at a temperature of 773 K with a holding time for 30 min under a pressure of 30 MPa. The composite was then annealed in vacuum at 873 K for various times to form various thicknesses of reaction zone. The formed reaction zone was identified as $WAl_{12}$ by a powder X-ray method. The fracture surfaces of the as-fabricated and annealed composites are shown in Fig. 4a and b, respectively. Interfacial reaction is not found in the as-fabricated composite (a). On the other hand, in the annealed composite (b), the formed brittle reaction zone exhibits multiple fracture, and debonding especially at the fibre/brittle zone interface is clearly found. Measured values of $\sigma'_c$ are shown in Fig. 5. Reduction in $\sigma'_c$ of the annealed specimens is relatively minor although the brittle zone is extremely thick, compared with that of the B/Ti40A and B/Ti75A composites. According to the rule of mixtures, as the brittle zone, being segmented, cannot carry the applied

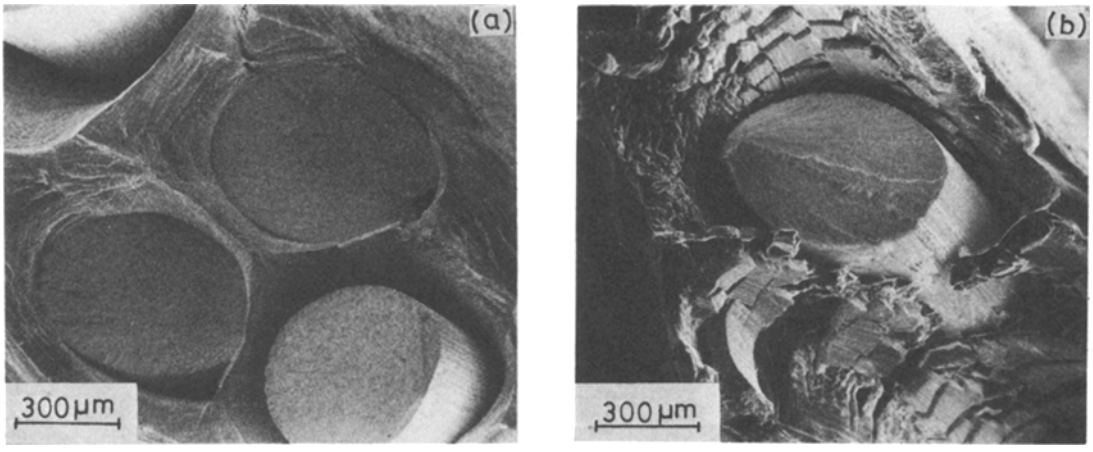


*Figure 4* Fracture surfaces of the (a) W/Al composite as-fabricated with $c = 0$, and (b) annealed with $c = 27\,\mu m$.

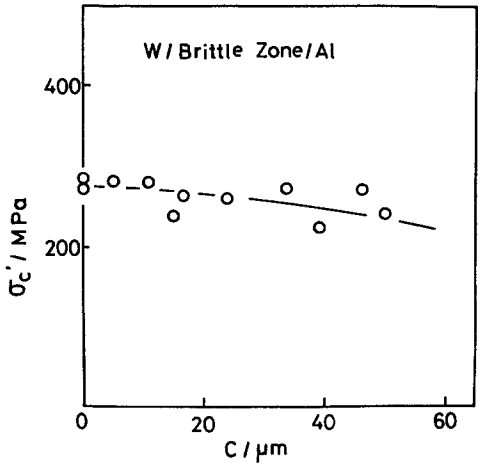


*Figure 5* Variations of $\sigma_c'$ of W/Al composite with $c$.

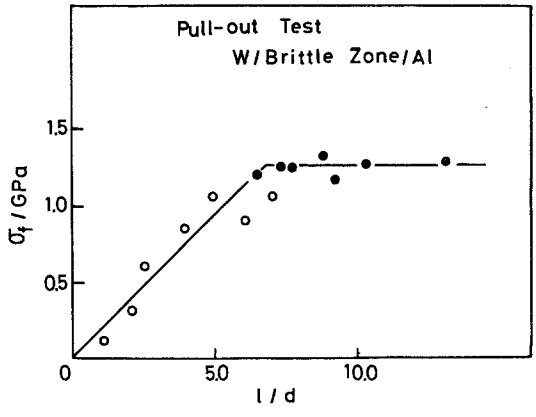


*Figure 6* Fibre stress $\sigma_f$ of W/Al composite with $c = 20\,\mu m$ at pull-out (open points) or fibre fracture (filled points) as a function of $l/d$.

load, the strength of the composite is given by

$$\sigma_c' = \sigma_{fu} V_f' + \sigma_m^* V_m', \qquad (33)$$

if the formed notches do not extend into the fibre. By substituting into Equation 33 the measured average values of $\sigma_{fu} = 1.29\,GPa$, $\sigma_m^* = 34.3\,MPa$, and $V_f'$, $V_b'$ and $V_m'$ measured as a function of $c$, a $\sigma_c'$ versus $c$ curve was calculated and superimposed (solid curve) on Fig. 5. The calculated curve fits well with the measured one. This result implies that the formed notch did not play a role in degrading the fibre strength.

The reason why the formed notch could not degrade the fibre is attributable to the weak interfacial bonding between the fibre and the brittle zone. To verify quantitatively this conception using the theory in Section 2.2, we should determine $\tau^{\Delta}$, $E_b$, $\sigma_{bu}$ and $\epsilon_{bu}$. $E_f$ is already known to be 412 GPa [15], and $V_f$ and $V_b$ of every specimen are measured experimentally.

First $\tau^{\Delta}$ was deduced by pull-out tests using the specimens containing a brittle zone of 20 $\mu m$ thick and by observation of the surface of the pulled-out fibre. Fig. 6 shows the stress in the fibre at pull-out (open points) or fibre fracture (filled points) as a function of the embedded length $l$ divided by the diameter $d$. The observation of the pulled-out fibre surface showed that the brittle zone adheres to the fibre in some parts (Fig. 7). This implies that debonding occurred at both the fibre/brittle zone and the brittle zone/matrix interfaces and the shear strength of both the interfaces was probably identical. As a result, $\tau^{\Delta}$ was determined to be 48.1 MPa.

$E_b$ and $G_b$ were assumed to be 80 GPa and 30 GPa respectively, since the chemical compo-

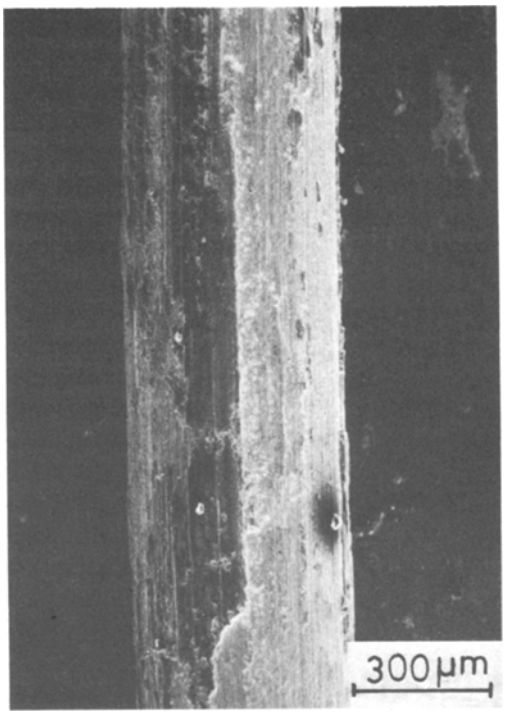


*Figure 7* The surfaces of the W fibre pulled-out from the W/Al composite with $c = 20\,\mu m$.

sition of the brittle zone is $WAl_{12}$ and, therefore, the elastic constants of the brittle zone might not be very different from aluminium.

$\sigma_{bu}$ was inferred from the multiple fracture of the zone in the following way. First we inferred that debonding at the fibre/brittle zone interface occurred prior to that at the brittle zone/matrix interface since the differences in the elastic constants between the fibre and the brittle zone were larger than those between the brittle zone and the matrix, and therefore stress concentration at the former interface should be higher than that at the latter. This inference seems to be supported by the fact that the brittle zone has completely detached from the fibre as shown in Fig. 4b. As a result, the multiple fracture of the brittle zone is considered to be a result of stress transfer from the matrix to the brittle zone. Applying Kelly's model [16] to this composite, the stress of the brittle zone $\sigma_b$ at a distance $z$ from the fractured part is given by

$$\pi(b^2 - a^2)\sigma_b = 2\pi b\tau z, \qquad (34)$$

where $\tau$ is the interfacial shear stress. By substituting $\sigma_b = \sigma_{bu}$, $\tau = \tau^{\Delta}$, and $z = l'$, where $l'$ is the average length of the segmented brittle zone, into Equation 34, $\sigma_{bu}$ is given by

$$\sigma_{bu} = 2b\tau^{\Delta}l'/(b^2 - a^2). \qquad (35)$$

For the specimen with $c = 50\,\mu m$, $a$, $b$ and $l'$ were measured as 0.24, 0.29 and 0.1 mm, respectively. Substituting these values and $\tau = 48.1$ MPa into Equation 35, $\sigma_{bu}$ was calculated to be 105 MPa. Then $\epsilon_{bu}$ was calculated to be 0.0013 by using the relation $\epsilon_{bu} = \sigma_{bu}/E_b$.

In order to know when debonding at the fibre/brittle zone interface occurred, $\epsilon_f^{\Delta}$ was calculated for all the specimens, using Equation 27. All the calculated values were smaller than $\epsilon_{bu}$. For instance, $\epsilon_f^{\Delta}$ was 0.000 87 and 0.000 88 for $c = 5$ and $50\,\mu m$, respectively, while $\epsilon_{bu}$ was 0.0013. This result implies that debonding occurs as soon as the brittle zone fractures, corresponding to case (a) in Section 2.2. Similarly, $\tau_{i,max}$ at the fracture of the brittle zone was calculated using Equation 24. As expected, all the calculated values were larger than $\tau^{\Delta}$. For instance, $\tau_{i,max}$ was 72 and 78 MPa for $c = 5$ and $50\,\mu m$, respectively, while $\tau^{\Delta}$ was 48.1 MPa.

In conclusion, in this composite, debonding at the fibre/brittle zone interface occurred immediately the brittle zone fractured. This debonding prevented the formed notch from extending into the fibre. Thus the fibre strength was not reduced and the loss of composite strength arose only from the reduction in effective cross-sectional area due to fracture of the brittle zone and decrease in fibre diameter.

### 3.3. Maximum permissible thickness of the brittle zone

As shown already, the fibre strength begins to decrease when the thickness of the brittle zone exceeds $c_I$. For $c < c_I$, the degrading effect by the formation of the notch is negligible compared to that of the intrinsic defects in the fibre. $c_I$ is regarded as the maximum permissible thickness. The $c_I$ for promising carbon, boron and silicon carbide fibres was calculated using Equation 8 in which $a$ was taken as the fibre radius. For silicon carbide fibre, $G_c^*$ was taken to be $45.9\,J\,m^{-2}$, since the fracture surface energy $\gamma_s (= G_c^*/2$ [17]) has been reported to be $22.9\,J\,m^{-2}$ [18]. For carbon fibre, $G_c^*$ was, to a first approximation, inferred using Equation 36

$$G_c^*/2 = \gamma_s = E_f a_o/20 \text{ [17]}, \qquad (36)$$

TABLE I The calculated values of the maximum permissible thickness, $c_I$, of the brittle zone for carbon, boron and silicon carbide fibres under the condition of strong interfacial bonding between the fibre and the zone, together with the values of $E_f$ (Young's modulus), $\sigma_{fu}$ (tensile strength), $G_c^*$ (critical strain energy release rate) and $a$ (fibre radius) which were substituted into Equation 8.

| | Carbon fibre | Boron fibre | Silicon carbide fibre |
|---|---|---|---|
| $c_I$ ($\mu$m) | 0.17 | 0.28 | 0.62 |
| $E_f$ (GPa) | 245 | 412 | 441 |
| $\sigma_{fu}$ (GPa) | 2.65 | 2.45 | 2.94 |
| $G_c^*$ (J m$^{-2}$) | 16.5 | 15.8 | 45.9 |
| $a$ ($\mu$m) | 3.43 | 50 | 50 |

where $a_o$ is the lattice spacing. In the calculation, $a_o$ was taken to be 0.67 nm [19]. For boron fibre, the value of $G_c^*$ obtained in Section 3.1 was again used. The values of $E_f$, $\sigma_{fu}$, $G_c^*$ and $a$ used, and the calculated values of $c_I$, are summarized in Table I.

All the calculated values of $c_I$ are smaller than 1 $\mu$m. This implies that interfacial reaction should be rigidly controlled during preparation and/or service. In general, in order to obtain good wetting between fibres and matrix, preparation should be carried out at high temperatures for long times, which in turn leads to excessive interfacial reaction. For practical preparation and service, coating might be inevitable to promote wetting and also to prevent the reaction.

In the above calculation, the fibre/brittle zone interface was assumed to be strong. However, in the case of weak bonding, notch effect will not arise due to premature debonding. Therefore, making the interfacial bonding weak might be another way of developing composite materials. This might be realized by addition of some element into the matrix in order to yield weak interfacial bonding. The fact that the interfacial bonding strength becomes weak [20] if the formation of the compound zone is forced to involve a reduction in volume, encourages us.

Of course, the above speculation should be applied only to the preparation technique for obtaining high-strength composites. If the interfacial bonding is weak, several problems arise with this. For instance, high transverse strength and good fatigue properties will not be achieved. How we can prepare excellent composites with high longitudinal and transverse strengths, high ductility, good fatigue properties, etc., is the subject for a further study.

Surface roughening on fibre surfaces, as well as the notch effect described in this paper, has been offered as an explanation for fibre degradation [21, 22]. The present theory is also applicable to surface roughening, as the roughness on fibre surfaces may possibly be regarded as the source of notches. In a qualitative manner, the permissible extent of surface roughness corresponds to $c_I$.

## 4. Conclusions

The strength of fibre-reinforced composites with brittle reaction zones was studied for both the cases of strong and weak interfacial bondings between the fibre and the brittle zone. A new model was proposed on the strength of composites. The proposed model was in fairly good agreement with the experimental results. By using the proposed model, the permissible thickness of the brittle zone, below which the strength of composites is not reduced, was calculated for some promising fibres. The calculated values of thickness were very small in the case of strong interfacial bonding. It was suggested that a coating or making the interface weak was one way for developing high strength composite materials when interfacial chemical reaction takes place in them.

## References


1. D. W. PETRASEK and J. W. WEETON, *Trans. Met. Soc. AIME* **230** (1964) 977.
2. P. W. HEITMAN, L. A. SHEPARD and T. H. COURTNEY, *J. Mech. Phys. Solids* **21** (1973) 75.
3. S. OCHIAI, M. MIZUHARA and Y. MURAKAMI, *J. Jap. Inst. Metals* **37** (1973) 208.
4. A. G. METCALFE and M. J. KLEIN, "Composite Materials", Vol. 1, edited by A. G. Metcalfe (Academic Press, New York and London, 1974) p. 125.
5. J. COOK and J. E. GORDEN, *Proc. Roy. Soc.* **282A** (1964) 508.
6. G. A. COOPER and A. KELLY, *J. Mech. Phys. Solids* **15** (1967) 279.
7. W. W. GERBERICH, *ibid* **19** (1971) 71.
8. S. OCHIAI and Y. MURAKAMI, *Trans. Jap. Inst. Metals* **18** (1977) 384.
9. S. OCHIAI, M. MIZUHARA and Y. MURAKAMI, *J. Jap. Inst. Metals* **41** (1977) 626.
10. H. TADA, P. PARIS and G. IRWIN, "The Stress Analysis of Cracks Handbook" (Del Research Corporation, Hellertown, Pennsylvania, 1973) p. 27.1.
11. *Idem, ibid* p. 1.12.
12. H. L. COX, *Brit. J. Appl. Phys.* **3** (1953) 72.
13. J. AVESTON and A. KELLY, *J. Mater. Sci.* **8** (1973) 352.
14. H. M. OTTE and H. A. LIPSITT, *Phys. Stat. Sol.* **13** (1966) 439.

15. C. J. SMITHELLS, "Metals Reference Book", Vol. 3 (Butterworth, London, 1967) p. 708.
16. A. KELLY, *Proc. Roy. Soc.* **282A** (1964) 63.
17. A. S. TETELMAN and A. J. McEVILY, Jr, "Fracture of Structural Materials" (J. Wiley, New York, 1967) p. 38.
18. J. R. McLAVEN, G. TAPPIN and R. W. DAVIDGE, *Proc. Brit. Ceram. Soc.* **22** (1972) 259.
19. B. E. BACON, *Acta Cryst.* **3** (1950) 320.
20. A. K. KURAKIN, *Fiz. Metal. Metalloved.* **30** (1970) 432.
21. J. L. CAMAHORT, *J. Comp. Mater.* **2** (1968) 104.
22. W. F. STUHRKE, "Metal Matrix Composites" (ASTM, Baltimore, 1968) p. 76.

Received 15 March and accepted 29 August 1978.